

Investigation of the chemical, strength, adhesion

by Cbm225 Sap

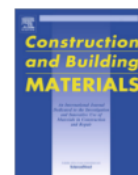
Submission date: 03-Sep-2020 07:02AM (UTC+0700)

Submission ID: 1378541959

File name: 1-s2.0-S0950061820313696-main.pdf (1.27M)

Word count: 7809

Character count: 39499



Investigation of the chemical, strength, adhesion and morphological properties of fly ash based geopolymer-modified bitumen



Sri Atmaja P. Rosyidi^a, Suzielah Rahmad^b, Nur Izzi Md. Yusoff^{b,*}, Aini Hazwani Shahrir^b, Ahmad Nazrul Hakimi Ibrahim^b, Nor Farah Nadia Ismail^c, Khairiah Haji Badri^d

^a Dept. of Civil Engineering, Universitas Muhammadiyah Yogyakarta, Yogyakarta, Indonesia

^b Dept. of Civil Engineering, Universiti Kebangsaan Malaysia, Selangor, Malaysia

^c Dept. of Civil Engineering, International Islamic University Malaysia, Kuala Lumpur, Malaysia

^d Department of Chemical Sciences, Universiti Kebangsaan Malaysia, Selangor, Malaysia

HIGHLIGHTS

- Chemical, strength, adhesion and morphology of GMB were investigated.
- Bitumen-geopolymer resulting the improvement in structural chain mobility properties.
- GMB has better resistance to moisture damage.
- Morphological changes in all GMB samples can be observed via AFM analysis.

ARTICLE INFO

Article history:

Received 27 October 2019

Received in revised form 24 April 2020

Accepted 25 April 2020

Keywords:

Fly ash
Geopolymer-modified bitumen
Chemical
Strength
Adhesion
Morphology

ABSTRACT

The current study seeks to investigate the chemical, strength, adhesion and morphological properties of fly-ash based geopolymer-modified bitumen (GMB). The geopolymer was prepared by mixing class F fly ash with alkaline solution (sodium silicate and sodium hydroxide), and was then mixed with an 80/100 penetration grade bitumen at different concentrations of 3, 5, 7 and 9% (by weight of bitumen) to produce the GMB. The chemical and strength properties of the binders were determined using the Fourier Transform Infrared Spectroscopy (FTIR) and Impact tests, respectively. The Surface Free Energy (SFE) and Atomic Force Microscope (AFM) tests were conducted to establish the adhesion and morphology of the binders. The modification of base bitumen with geopolymer resulting the improvement in structural chain mobility properties and improved storage stability compared to those of the control sample. The result of FTIR analysis showed that the incorporation of geopolymer into base bitumen did not cause any change in the functional groups, where the peaks of aromatic C=C stretching is at around 1600 cm⁻¹ (stretch), 1475 cm⁻¹ (stretch) and 900–600 cm⁻¹ (out-of-plane bend). The peak at around 1390 cm⁻¹ clearly shows the stretch of the C-N amine group. The result of SFE test shows that GMB has better resistance to moisture damage. Finally, the AFM analysis revealed morphological changes in all GMB samples. In general, the addition of 5% geopolymer can be considered as is the optimum concentration for bitumen modification.

© 2020 Elsevier Ltd. All rights reserved.

1. Introduction

The incorporation of polymers, which are repeating chains of small molecules, to bitumen has been demonstrated to enhance pavement performance. Polymer-modified bitumen (PMB) has a

higher rutting and thermal cracking resistance and reduced fatigue damage, stripping and temperature susceptibility [1]. PMB has been used with success at high-stress locations, including at the junction of busy streets, airports, vehicle weighing stations and race tracks [2]. A large number of polymers, including polyethylene and polyolefin, have been investigated to determine the feasibility of using them as a bitumen modifier. However, more attention was given to styrene homo-polymers and copolymers, ionomers, ethylene-vinyl acetate and acrylic, rubbers, polymer blends and other polymeric materials [3]. More recently, researchers also have

* Corresponding author.

E-mail addresses: atmaja_sri@umy.ac.id (S.A.P. Rosyidi), izzi@ukm.edu.my (Nur Izzi Md. Yusoff), norfarahnadia@iiu.edu.my (N.F.N. Ismail), kaybadri@ukm.edu.my (K.H. Badri).

been focusing their attention to the feasibility of using recycled or scrap plastics [4], including tire-rubber crumb [5], to modify bitumen. Recycled materials, such as recycled asphalt pavement, can be used as pavement material after they have been stabilised with cement or chemically stabilised. The use of waste by-products in engineering infrastructure has been shown to be a more feasible alternative to the use of excavated materials [6], and thus contribute to conserving energy and natural resources. However, there is an urgent need to find alternative green materials for cement due to its negative impact on the environment. One of the materials that can be used to replace cement is fly ash (FA) based geopolymer, which is an eco-friendly additive that has the ability to impart superior mechanical properties than Portland cement [7].

The term geopolymer was first used by Davidovits [8] to characterise alternative cementitious materials with ceramic-like properties. Geopolymers are frequently mistaken as the alkali-activated cements developed in the 1950s by Glukhovskiy in Ukraine [9]. The inorganic framework of geopolymers imparts them with fire resistance properties and outstanding thermal stability in comparison to traditional cements [10]. The mechanical properties of geopolymer surpasses those of Ordinary Portland Cement (OPC) [11–13]. Because fly ash-based geopolymer is an industrial waste, its production is more energy efficient than that of OPC [14]. The technology for producing geopolymer does not require high-temperature calcining and therefore is able to reduce emission by 80% [8]. Previous studies on the use of geopolymer tend to give more focus to its effects in various uses, particularly in the production of composite materials [8,15–18]. It is used as fire and heat-resistant coatings and adhesives, for medical application, as high-temperature ceramics, as binders for fire-resistant fibre composites, for the encapsulation of toxic and radioactive wastes, and as a new type of cement for concrete [19]. Zain et al. [20] conducted a comparative study of fly ash, metakaolin, kaolin, palm oil flying ash, and dolomite-based geopolymer material and found that fly ash based geopolymer has the highest efficiency when used in silicon oxide (SiO_2) and aluminium oxide (Al_2O_3) composites. The researchers were also able to demonstrate that the reuse of coal waste products in fly ash based geopolymer contribute to the conservation and sustainability of the environment. Investigations are being carried out on the feasibility of using geopolymer in various scientific and industrial fields, including modern inorganic chemistry, physical chemistry, colloid chemistry, mineralogy, geology, as well as in various engineering process technologies. The possibility of using geopolymer in pavement structural layers is also being explored [21,22].

For example, Hoy et al. [21,22] investigated the use of a low-carbon stabilisation method by using Recycled Asphalt Pavement (RAP) and Fly Ash (FA) geopolymers as road base material. The result of Toxicity Characteristic Leaching Procedure (TCLP) showed that the use of RAP-FA blends and RAP-FA geopolymers in the construction of road pavements do not pose any hazard to the environment [21]. Results also showed that FA-geopolymer has the ability to considerably enhance the Unconfined Compression Strength (UCS) and durability of RAP-FA blend [22]. Poltue et al. [18] investigated the use of fly ash (FA) and rice husk ash (RHA) based geopolymer to enhance the compressive strength of recycled concrete aggregate (RCA) used as a lightweight stabilised pavement base material. The study has demonstrated the prospective of using FA-RHA-geopolymer stabilised RCA as an alternative stabilised road base material. Recently, Ibrahim et al. [23] have demonstrated a good compatibility of geopolymer with bitumen. The addition of geopolymer to bitumen resulted in improved permanent deformation resistance of the binder [23]. Another study by Ali et al. [24] have shown that FA is able to enhance resilient modulus characteristics and stripping resistance when used as a mineral filler. Even though the incorporation of FA did not result

in a considerable reduction of field performance of asphalt mixture with regard to permanent deformation and present serviceability index (PSI), there was a greater degree of surface cracking on the road surface.

A review of the literature showed that there is scarce research on the use of geopolymer materials as a modifier for bitumen and asphalt mixture [25]. Therefore, this study aims to investigate the chemical, strength, adhesion and morphological properties of a 80/100 penetration grade bitumen modified with FA based geopolymer in order to produce the optimal geopolymer-modified bitumen (GMB). Five bitumen samples were modified with geopolymer at different percentages of 0, 3, 5, 7 and 9% (by weight of bitumen). The samples were then subjected to physical testing, namely penetration, ductility, softening point, viscosity and storage stability tests. In addition, the Fourier Transform Infrared Spectroscopy (FTIR) and Impact tests were carried out to determine the chemical and strength properties of the base bitumen and GMBs. Finally, adhesion and morphological analyses were done using Surface Free Energy (SFE) and Atomic Force Microscope (AFM) tests.

2. Experimental design

2.1. Materials

The binder used in this study has a 80/100 penetration grade bitumen with a specific gravity of 1.03. This bitumen was provided by the Cenco Science Company, a bitumen factory in Port Klang, Malaysia. The fly ash was provided by the Kapar Power Station located in Selangor, Malaysia and, based on the ASTM C 618, is a class F fly ash. This fly ash has a specific gravity of 2.26 and its chemical composition is presented in Table 1.

The geopolymer material was obtained through a reaction between fly ash and an alkaline activator. The alkaline activator used in the present study is a combination of sodium hydroxide (NaOH) solution and sodium silicate (Na_2SiO_3) solution with with $M_s = 2.0$ (Na_2O : 14.73%; SiO_2 : 29.75% and H_2O : 55.52%). The NaOH is in pellet form and has a purity of 99%. It was dissolved in distilled water to obtain a 8 M NaOH solution.

2.2. Sample preparation

The base bitumen was heated at 150 ± 5 °C until it becomes liquid, and the geopolymer gel was then added to the binder. The materials used for preparing the geopolymer gel are fly ash, NaOH solution and Na_2SiO_3 solution. The ratio of fly ash to alkaline activator is 0.45, and the ratio of Na_2SiO_3 solution to NaOH solution is 2.5. The Na_2SiO_3 and NaOH solutions were kept for 24 h in airtight canister after mixed by mechanical mixing for 90 min at a mixing speed of 1000 ± 10 rpm and a temperature of 150 ± 5 °C [5]. These ratio was chosen based on previous studies done by Ibrahim et al. [26] and Kusbiantoro et al. [27]. The geopolymer was added to the

Table 1
Chemical composition of the fly ash (%).

Oxide	Value
SiO_2	52.50
Al_2O_3	22.82
Fe_2O_3	5.34
CaO	7.16
MgO	2.56
SO_3	0.20
K_2O	0.99
Na_2O	0.48
LOI	3.35

bitumen at various percentages of 0, 3, 5, 7 and 9% (by weight of bitumen). The samples were named based on the percentage of geopolymer; for example, the sample with 3 and 5% of geopolymer are named GMB3 and GMB5, respectively. Table 2 shows the physical properties of the base bitumen and GMBs.

Results of laboratory tests showed that the incorporation of geopolymer into bitumen resulted in enhanced elastic properties of the bitumen. This is evident by the higher hardness, softening point temperature, and viscosity values compared to those of the base bitumen. The characterisation of physical properties showed that GMB5 has the greatest improvement in physical properties.

2.3. Fourier Transform Infrared Spectroscopy test

Fourier Transform Infrared Spectroscopy (FTIR) was used to identify the functional group peaks and bonding of the geopolymer, base bitumen and GMB samples [28]. The FTIR was performed using the Perkin Elmer Spectrum GX spectrophotometer. Samples were analysed over wave numbers 4000 cm^{-1} to 650 cm^{-1} using the Attenuated Total Reflectance (ATR) method.

2.4. Impact test

Notched Izod Impact is a single point test which measures the resistance of a material to the impact imposed by a swinging pendulum. The Izod method was conducted on a $60\text{ mm} \times 12\text{ mm} \times 3\text{ mm}$ unnotched sample. Prior to testing, each specimen was instantly frozen by using liquid nitrogen. The force of the Izod Impact Machine pendulum used for this test was 2.7609 J. The impact strength of the bituminous binder was calculated by dividing the impact energy with the sample cross sectional area, and the average of three readings was recorded as the impact strength. The outcome of this test is expressed as kinetic energy (E) in Joule (J). Higher impact strength values indicate tougher material. This test was done in ambient temperature of $23 \pm 3\text{ }^\circ\text{C}$ in a closed space of a fully air conditioned laboratory, in accordance to ASTM D256.

2.5. Surface free energy test

The Surface Free Energy (SFE) test was used to evaluate adhesion properties through a combination of aggregate surface free energy in the presence of water, which is related to moisture degradation of asphalt pavements. The contact angle approach was used to determine the bitumen's SFE. The value of the contact angle was determined using the sessile drop technique. This experiment was done using a Goniometer device. Three different probe liquids, distilled water, formamide and glycol, were used in the contact-point experiments due to their large surface free energy and varying free surface components [29]. A device camera was used to capture a direct image of the drop on the sample surface and the contact angle between the fluid and the sample was measured. The assessment was done in a controlled environment chamber. Each liquid was dropped at three different locations on

the bitumen film and the contact angle was measured. The average contact angle was recorded for further analysis.

2.6. Atomic Force Microscope test

The Atomic Force Microscope (AFM) test was used to analyse the adhesion strength of the base bitumen and GMBs. AFM power mapping was done to determine the adhesive properties of bitumen. The tip of the silicone needle in the AFM represent the silicone mineral in the aggregate and is in contact with the surface of the bonding agent. The analysis used the contact mode to determine the microscale topography of the samples. The AFM tip, which was attached to the low spring constant cantilever arm, made a gentle "physical contact" with the sample atoms. As the tip slowly scan the sample, the force of contact caused the cantilever to bend to adapt to any change in the topography. The curve was plotted during the approach and retraction of the needle. The size and strength of bitumen adhesion was measured based on the obtained curve. In this curvature test, the peak force is taken as the contact force between the silicon needle and bitumen surface. In order to minimise the damage to the original bitumen structure the peak force is set to a very small value of 5 nN.

3. Results and discussion

3.1. Chemical properties

Fig. 1 shows the FTIR spectra of the bitumen, geopolymer, and geopolymer modified bitumen. The FTIR spectrum in Table 3 shows that the peaks of aromatic C=C stretching are at around 1600 cm^{-1} (stretch), 1475 cm^{-1} (stretch) and $900\text{--}600\text{ cm}^{-1}$ (out-of-plane bend). The peak at around 1390 cm^{-1} clearly shows the stretch of C-N amine group. The C-O group stretching is at about 1050 cm^{-1} . The peak stretch of C=N amine group overlaps with that of the aromatic C=C (1600 cm^{-1}) due to its weaker signal than the peaks of aromatic C=C. The remaining peaks between 3000 and 2800 cm^{-1} are the stretching peaks for the alkyl group C-H.

Geopolymers contain various metal components, including aluminium, silicon, and potassium, that makes the geopolymer materials used in this study unsuitable for analysis by FTIR spectroscopy techniques. The more appropriate technique for analyzing geopolymer is by using far infrared (a range $>600\text{ cm}^{-1}$). This allows for the observation of the peak of sulphur trioxide (SO_3) stretch at about 950 cm^{-1} in the geopolymer's FTIR spectrum. The remaining peaks are due to the impurities or moisture pollution that depends on the degree of permeability of the obtained peaks is too wide in the FTIR spectrum of the geopolymer.

The addition of geopolymer did not produce any significant change in the FTIR spectrum, indicating that there is no change in the functional group of the bitumen. This could be due to the incorporation of insufficient amount of geopolymer (less than 10%) which did not have a significant impact on the geometry of FTIR spectrum of the modified bitumen. It is also possible that

Table 2
Physical properties of base bitumen and GMBs.

Property	Percentage (%)					Testing Standard
	0	3	5	7	9	
Penetration at $25\text{ }^\circ\text{C}$	84	76	61	68	71	ASTM D5
Ductility, cm	150	126	100	91	118	ASTM D113
Softening point, $^\circ\text{C}$	47.0	49.0	56.5	53.0	49.5	ASTM D26
Viscosity at $135\text{ }^\circ\text{C}$, Pa.s	0.36	0.42	0.46	0.43	0.43	ASTM D4402
Viscosity at $160\text{ }^\circ\text{C}$, Pa.s	0.12	0.13	0.17	0.14	0.14	ASTM D4402
Storage Stability, temperature difference $^\circ\text{C}$	0	1.0	0	1.0	0	ASTM D5976

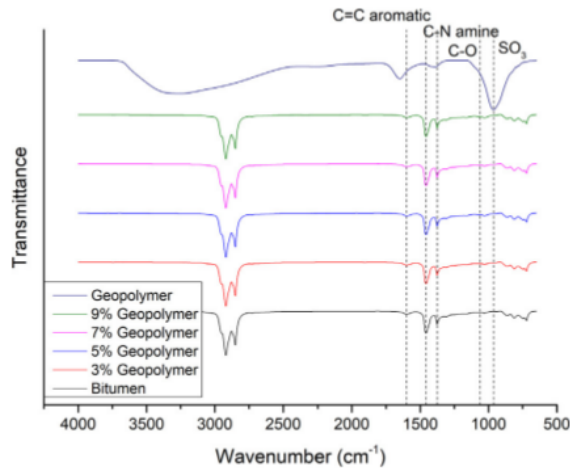


Fig. 1. FTIR spectra of base bitumen, geopolymer, and GMBs.

the absorption peak of the geopolymer material overlaps with the sharp or wider bitumen absorption peak because of the higher amount of bitumen used. Moreover, the reaction that occurs in the bitumen modification process was observed physically but not chemically.

3.2. Impact resistance

Fig. 2 shows the impact values for the base bitumen and GMBs. Results show that the impact strength of GMB3 and GMB5 increased to 2.38 kJ/m² and 3.27 kJ/m², respectively, compared to the control sample value of 1.58 kJ/m². The increase in impact strength is due to the shear structure of the chain on the filler's surface which affluences the matrix structure involved [30]. However, the impact strength of GMB7 decreased slightly to 2.90 kJ/m². The incorporation of higher amounts of geopolymer to the base bitumen (GMB9) resulted in a considerable reduction of the impact strength to 1.59 kJ/m². The reduced impact strength value is very apparent, and is closely related with the amount of modified material in the binding matrix. According to Amin and Badri [31], the addition of excessive amount of filler produced a fragile composite sample that break easily. The strength of the modified binders is influenced by the percentage of geopolymers incorporated to the base bitumen.

3.3. Adhesion properties

The SFE of the binder and aggregate bonds can be used to evaluate adhesive work through a combination of SFE in the presence of liquid which is related to the moisture degradation of asphalt pavements. A good bitumen-aggregate adhesion improves mixing properties and ensure a more durable mixing structure [32]. Therefore, it is critical to determine the SFE of the bitumen and

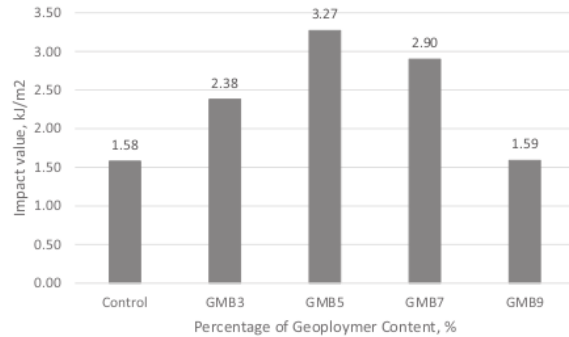


Fig. 2. Impact values of base bitumen and GMBs.

aggregates. One proven method for estimating bitumen's SFE is through the contact angle approach by using several different probe liquids [29]. This study used the sessile drop method and different probe liquids to measure the contact angle between the liquids and solid surface (bitumen) due to the simplicity of the method. Following this the surface free energy was determined using the Owen-Wendt equation (Eq. (1)):

$$\gamma_{sl} = \gamma_s + \gamma_l - 2\sqrt{\gamma_s^d \gamma_l^d} - 2\sqrt{\gamma_s^p \gamma_l^p} \quad (1)$$

which can be deduced into:

$$\frac{(1 + \cos \theta)}{2} \frac{\gamma_l}{\sqrt{\gamma_l^d}} = \sqrt{\gamma_s^p} \times \sqrt{\frac{\gamma_l^p}{\gamma_l^d}} + \sqrt{\gamma_s^d} \quad (2)$$

Plotting $[(1 + \cos \theta)/2] (\gamma_l/\sqrt{\gamma_l^d})$ against $\sqrt{\gamma_l^p/\gamma_l^d}$ gives a straight line. The polar part, γ_s^p is the square of the plot while the dispersion part γ_s^d is the square of the intercept.

3.3.1. Contact angle

Table 4 shows the average value of the largest contact angle of the base bitumen and GMB samples measured using water (92–98°), formamide (76–91°), and glycol (80–87°) as a probe liquid. It should be noted that since this experiment was conducted in a controlled environment chamber, there is a strong relationship between the bitumen and the probe liquids. Grenfell et al. [33] stated that the higher the value of the contact angles between the solid surface (bitumen) and the liquid, the lower the potential for both to adhere to one another. In general, a contact angle greater than 90° is more likely to be hydrophobic. Therefore, the experimental results shown in Table 4 support the general perception that bitumen is naturally hydrophobic when applied with water.

However, Table 4 also shows different results for formamide and glycol. The highest contact angle when using formamide on the GMB5 sample is 90.17°, whereas all contact angles between the liquids and the control bitumen and modified bitumen samples when using glycol are less than 90°. This indicates that the base bitumen and geopolymer-modified bitumen used in this experiment have a

Table 3
Functional peak groups of base bitumen, geopolymer and GMBs.

Peak Absorption/Stretch	Wave number, cm ⁻¹					
	Bitumen	Geopolymer	GMB3	GMB5	GMB7	GMB9
C=C aromatic	1600, 1457	–	1600, 1457	1600, 1456	1600, 1457	1601, 1457
C-N amine	1376	–	1376	1376	1376	1376
C-O	1061	–	1061	1059	1060	1057
C-H	2951	–	2950	2951	2951	2951
S	–	963	963	963	963	964

Table 4
Contact angles of base bitumen and GMBs.

Sample	Contact Angle Average (°)		
	Water	Formamide	Glycol
Base bitumen	94.93	86.87	86.57
GMB3	95.43	76.08	82.97
GMB5	93.13	90.17	80.75
GMB7	97.58	86.93	82.33
GMB9	92.63	83.05	81.37

high tendency to adhere to formamide and glycol. In addition, the contact angles in this experiment are used to measure the properties of bitumen surface and probe liquids. The small contact angles indicate that the liquids used can effectively wet the surface of the bitumen, while large contact angles show poor wettability [34].

Additionally, Table 4 shows that all base bitumen and geopolymer modified bitumen samples have high contact angles when water was used as the probe liquid. The GMB7 sample has the largest contact angle, indicating that the addition of 7 percent geopolymers to the base bitumen resulted in reduced surface properties of bitumen to water while increasing the waterproof properties of the bitumen. However, smaller contact angles were obtained when formamide and glycols were used as probe liquids. The use of formamide resulted in a higher contact point when 5% geopolymer was added to the base bitumen although the contact angle decreased when the percentage of geopolymers was increased to 7 and 9%. The use of glycol resulted in smaller contact angle when higher percentages of geopolymer were incorporated to the base bitumen.

A method developed by Kwok [35] was used to assess the validity of the results for contact angle. The relationship between $\gamma l \cos \theta$ and γl for the solid samples used with different liquid probes must be linear, where γl is the surface free energy (SFE) of the liquid used to determine the contact angle and θ is the contact angle between the solid surface and the liquid. If the resulting curves do not match, the results of the experiment have to be re-evaluated. The graphs of $\gamma l \cos \theta$ against γl for the base bitumen and each of the geopolymer-modified bitumen sample in this experiment are linear and the coefficient of determination (R^2) range from 0.48 to 0.95. This indicates that the contact angles obtained in this experiment have met the requirement stated in previous studies, and thus the selection of distilled water, formamide and glycol as probe liquid is appropriate [36]. Table 5 shows the correlation

Table 5
Coefficient of determination between $\gamma l \cos \theta$ and γl .

Sample	Coefficient of Determination (R^2)
Base bitumen	0.8183
GMB3	0.4784
GMB5	0.9066
GMB7	0.9541
GMB9	0.8502

Table 6
Surface energy of base bitumen and GMBs and Coefficient of determination between $[(1 + \cos \theta)/2] (\gamma l / \sqrt{\gamma} l d)$ and $\sqrt{\gamma} l d / \gamma l d$.

Sample	Surface Free Energy (mj/m ²)			Coefficient of Determination (R^2)
	Total, γ	Dispersion, γ^{LW}	Polar, γ^{AB}	
Base bitumen	15.41	6.86	8.55	0.9646
GMB3	18.03	13.36	4.67	0.6960
GMB5	16.41	6.09	10.32	0.9958
GMB7	15.76	10.43	5.33	0.9979
GMB9	17.32	9.03	8.29	0.9757

coefficients of $\gamma l \cos \theta$ and γl for the base bitumen and geopolymer-modified bitumen samples.

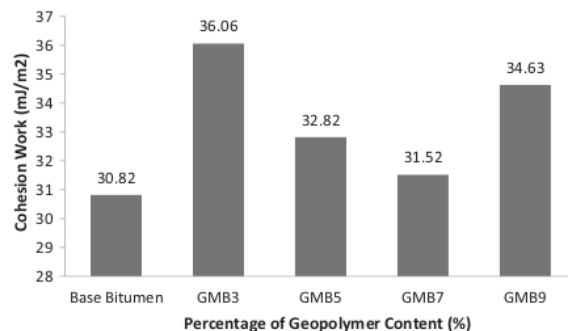
3.3.2. SFE

Table 6 shows the relationships between $[(1 + \cos \theta)/2] (\gamma l / \sqrt{\gamma} l d)$ and $\sqrt{\gamma} l d / \gamma l d$ where the R^2 for the control sample and GMBs range from 0.696 to 0.9979. In other words, the variation in the SFE is due to variation in the contact angle which range from 70 to almost 100 percent.

Even though this does not necessarily mean that the contact angle has a real effect on SFE, it appears to be so. This indicates that the results obtained in this experiment are valid. Table 6 shows the SFE for the control and GMBs samples together with the free energy components calculated using the following formula, $[(1 + \cos \theta)/2] (\gamma l / \sqrt{\gamma} l d) = \sqrt{\gamma} sp \times \sqrt{\gamma} lp / \gamma l d \times \sqrt{\gamma} sd$. According to Fowkes [37], the square root of the graph slope is the value of γsp , while the square root of the intersection on the y-axis is the value γsd . The total SFE of the base bitumen and GMB samples range from 15.41 to 18.03 mj/m². While almost all of the values of dispersion components are dominant over the polar component values, with the exception of the base bitumen and GMB5, these findings support the results obtained by Hefer et al. [29] and Hubbe et al. [36].

3.3.3. Cohesion and work of adhesion

The work of cohesion of bitumen is the energy that separate bitumen from one unit of an area into two new surfaces, while work of adhesion is the energy that separate the bitumen bond from the aggregate interface. This test was done at an ambient temperature of 23 ± 3 °C in a closed space of a fully air conditioned laboratory. Fig. 3 shows the work of cohesion for the base bitumen and GMB samples. The highest recovery value was observed for the GMB3 sample. At 5 and 7% geopolymer content, the work of cohesion decreased slightly; this could be because the foaming of the bitumen weakened the work of debonding of the system [38]. However, the work of cohesion increased again at 9% geopolymer content. The values for the GMB samples are higher than that for

**Fig. 3.** Work of cohesion of base bitumen and GMBs.

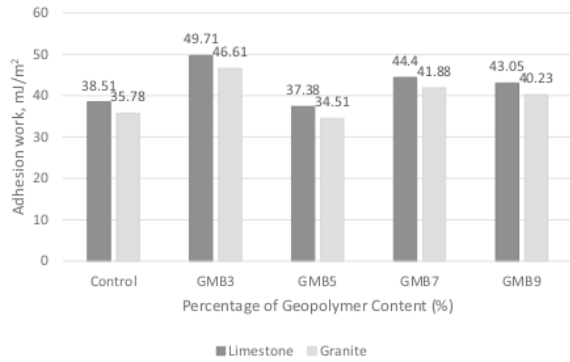


Fig. 4. Work of adhesion of aggregates and bitumen in dry condition.

base bitumen samples, indicating that the addition of geopolymer increased the workability of bitumen in bonding. The high work of cohesion value of bitumen indicates good resistance to cracking. These results illustrate the positive effects of geopolymer modification on the work of cohesion on bitumen surface in the absence of water.

The values for work of adhesion of each aggregate (limestone and granite) and bitumen combinations in dry condition are shown in Fig. 4. GMB3 has the highest work of adhesion value. However, the value decreased at 5% geopolymer content, increased at 7% geopolymer content, and decreased again at 9% geopolymer content. The work of adhesion of all GMBs are higher than the that for the control sample, with the exception of GMB5 which showed a slightly lower work of adhesion compared to the control bitumen. This result suggests that 3% geopolymer is the optimum extraction percentage for improving the bitumen's work of adhesion.

The adhesion value of combined bitumen and aggregates in the presence of water is shown in Fig. 5. The negative value in the graph indicates that the presence of water has caused debonding along the interface. Higher magnitudes indicate higher energy potential to disrupt the bonding of bitumen and aggregate in the presence of water. The results shown in Fig. 5 suggest that GMB5 is less susceptible to moisture damage compared to the other samples. The small adhesion value suggests that the moisture damage susceptibility of the limestone-bitumen combination is better than that of granite-bitumen combination. In general, the addition of geopolymer to both aggregates (limestone and granite) resulted in less work of adhesion in the presence of water; this is proven by the results for the GMB3 and GMB7 samples.

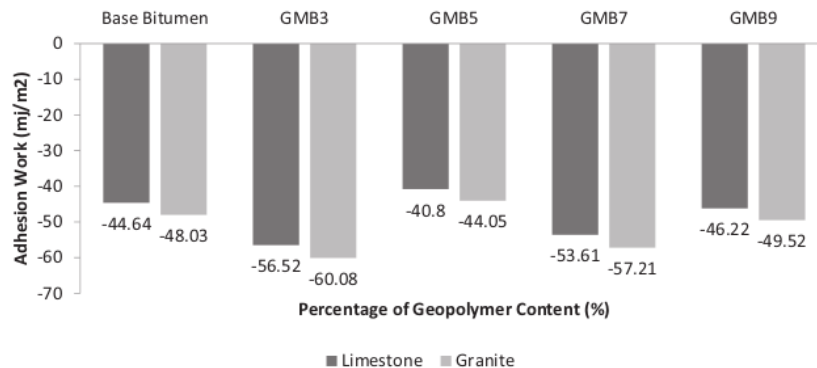


Fig. 5. Work of adhesion of aggregates and bitumen in the presence of water (wet).

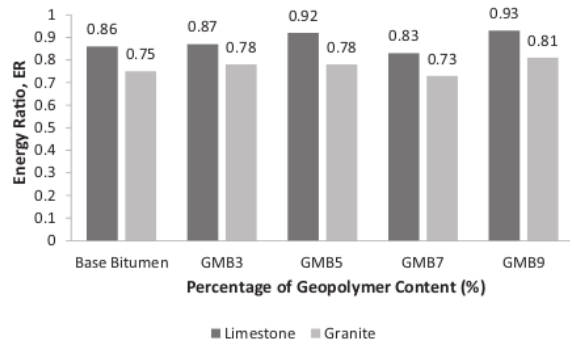


Fig. 6. Comparison of energy ratio.

Fig. 6 shows the value of energy ratio, ER, calculated based on the value the work of adhesion. Basically, ER is the ratio of wettability of the surface ($W_{AB} - W_{BB}$) to the work of adhesion in wet condition (W_{ABW}^{wet}) [39]. The value of ER was calculated using Eq. (3):

$$ER = \left| \frac{(W_{AB} - W_{BB})}{W_{ABW}^{wet}} \right| \quad (3)$$

Based on the values shown in the diagram, the susceptibility to moisture degradation can be reduced by adding geopolymer to bitumen. GMB9 has the highest energy ratio, indicating that higher geopolymer percentages are able to improve susceptibility to moisture damage.

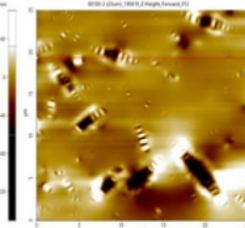
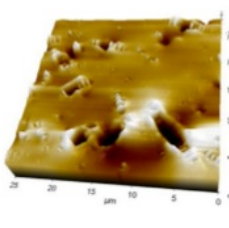
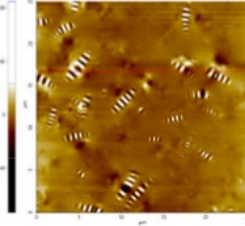
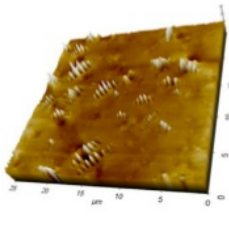
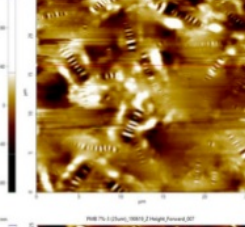
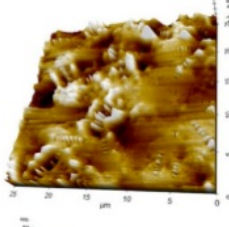
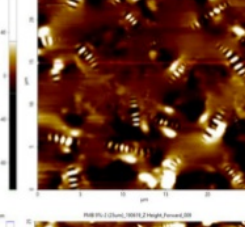
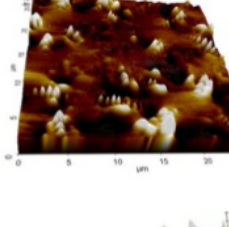
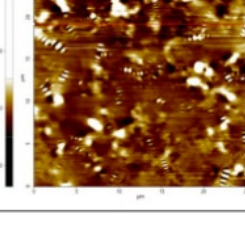
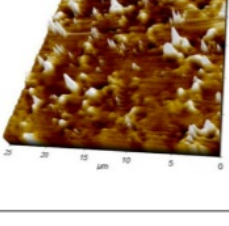
3.4. AFM

AFM is a very important tool in the assessment of bitumen. Binning et al. [33] was the first researcher to use AFN to measure binder's surface topography and surface strength. In this study the characteristics of bitumen samples was established through AFM. Pauli et al. [40] employed AFM to characterise the component of bitumen and its properties.

3.4.1. Topography

Table 7 shows the two-dimensional (2D) and three-dimensional (3D) images and topographic profiles of the base bitumen. The 2D image shows the presence of a flat surface background interspersed with a phase of dark colour. This phase includes long structures characterised by white and black stripes. According to Loeber et al. [41,42] the phase with the white and black line is known as the bee structure. Bo et al. [43] stated that binders are complex

Table 7
Comparison of 2D and 3D images of base bitumen and GMBs.

Geopolymer Content (%)	2D Image	3D Image
Base bitumen		
3		
5		
7		
9		

materials made up of a combination of hydrogen and carbon (hydrocarbons). The majority of bonded binders are made up of heteroatoms such as sulphur, nitrogen and oxygen. In addition, the metal content of titanium binders, including vanadium, nickel and iron, is less than 1%. Bitumen molecule which contains aliphatic aromatic substances and aromatic structures are categorized as asphaltene or maltene depending on whether they dissolve in hexane or heptane. The bee structure shown in Table 7 is associated with the presence of asphaltene [44]. Masson et al. [45], however, disagree with this assessment given the strong association of the areas of bee structure with the amount of vanadium and nickel in the bitumen.

The topographic profile shows vertical fluctuations of the sample. Five topographic profiles were measured throughout the control bitumen and GMB samples and the results are shown in Table 7. The distance between the highest peaks and the lowest valleys was evaluated and results show that the topographic profiles of the five bitumen samples are different. As can be seen, the sample surface of the base bitumen and the GMB3 is brighter and more flat compared to those of GMB5, GMB7 and GMB9 which have a darker and coarser surface. The bee structure of the base bitumen and GMB3 are smaller with smaller valley value compared to those for GMB5, GMB7 and GMB9. The topographic images show that higher percentage of geopolymer contribute to

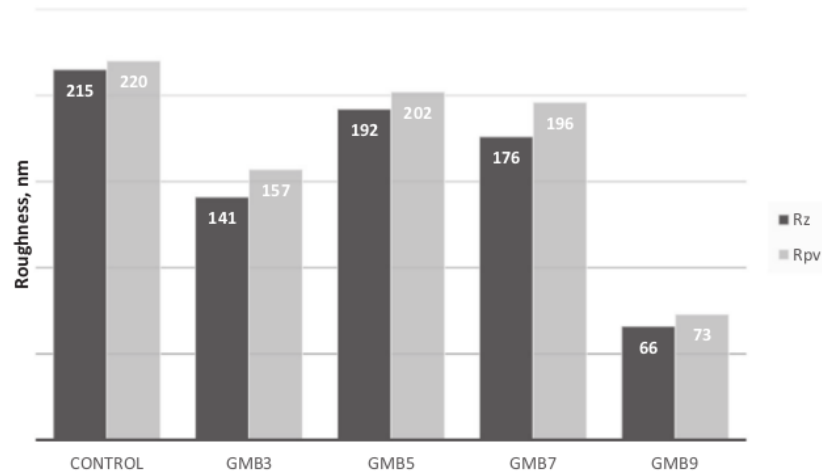


Fig. 7. Roughness parameter values of base bitumen and GMBs.

the increase of bee structure on the sample surface. It is assumed that the high stiffness of the bee structure is caused by the presence of asphaltene and resin [44]. In addition, the topographic profile in Table 7 shows that as the percentage of geopolymer increased, the surface structure in the topography profile decreased dramatically. Therefore, it can be concluded that asphaltene contributes to the peak height of the bee structure, indicating that increasing the percentage of geopolymer also contributes to higher asphaltene content in the bitumen.

The 3D image in Table 7 provides a better view of the height of structure on the surface of the sample. In the three-dimensional image (3D) the height mode is used to generate the same effect as the two-dimensional image (2D). The colours of the peaks and valleys seen on the 3D surface differ, where white represents higher surface while the darker colours represent the lower valleys. The highest peaks were observed at 5, 7 and 9% geopolymer content, which correspond with the topographic images and profiles. The bee structures observed in the 2D image is seen as bulbs in the 3D image. The bee structure in the 3D image is derived from the highest peaks and valleys on the topographic surface and is surrounded by a flat surface matrix. In addition, the 3D image shows that the bee structure in GMB5, GMB7 and GMB9 samples are significantly larger compared to control bitumen and GMB3 samples. This may be attributed to the aggregation of wax crystals as a result of the lower melting temperature; McCarron et al. [46] have shown that at higher temperature the wax crystals melted back into the matrix phases of the bitumen and thus uniformly reduce the size and shape of the bee structures. The large number of bumps can be attributed to the significant fluctuations in the surface structure of the topographic profile in the 2D images. The bulbs on the surface of this sample can be attributed to asphaltene. The high number of bumps in the GMB5, GMB7 and GMB9 samples may be attributed to the asphaltene contents in the three samples.

3.4.2. Roughness

The roughness of bitumen is a representation of the bitumen's corrugated microstructure surface. Roughness or height fluctuation can be calculated using a number of parameters. The parameter chosen is dependent on the aim of the analysis. It can be either the valley quantification, mean height, or peak quantification. In this study, the roughness of the samples was determined by the average value of the five highest peaks or lowest valleys on the sample surface. Fig. 7 shows the values of the R_z and R_{pv} parameters obtained through AFM topography. R_z is the average value of

the ten roughness points in the topographic profile, which is the arithmetic average value of the five highest peaks or lowest valleys on the sample surface. R_{pv} is the peak-to-valley value, which is the ratio of the highest and lowest peaks of the sample surface. The base bitumen sample has the highest R_z value of 215 nm, while GMB9 has the lowest R_z value of 66 nm. This is because the base bitumen has the highest peak value and the lowest peak compared to other GMB samples. Therefore, asphaltene content and bee structure have a great influence on surface roughness, similar to those observed in the 3D topography and images.

4. Conclusions

Several conclusions can be drawn from this study:

- The functional groups for base bitumen, geopolymer and GMBs were determined via FTIR analysis. The addition of geopolymer did not produce any significant change in the FTIR spectrum, indicating that there is no change in the functional groups after bitumen modification with geopolymer. This could be due to the small amount of geopolymer (less than 10%) not having a considerable impact to the geometry of modified bitumen's FTIR spectra.
- The addition of geopolymer resulted in higher impact values of the modified bitumen in comparison to the base bitumen. The highest impact value was recorded for GMB5. The SFE values for base bitumen and the GMB samples ranged from 15.41 to 18.03 $\text{mJ}\cdot\text{m}^{-2}$. Nearly all dispersion component values are dominant over polar component values except for the control sample and GMB5. GMB3 has the highest work of adhesion value when combined with limestone and granite.
- AFM characterisation through observation of the topography, 3D images and surface roughness showed that the incorporation of higher percentages of geopolymer in bitumen resulted in a higher asphaltene content and enhanced bee structure of the binder. Overall, GMB5 showed the best results and thus 5 percent geopolymer content is assumed to be the optimum concentration for bitumen modification.

CRedit authorship contribution statement

Sri Atmaja P. Rosyidi: Writing - review & editing, Supervision. **Suzielah Rahmad:** Writing - review & editing, Investigation, Visualization. **Nur Izzid Md. Yusoff:** Writing - review & editing, Supervision.

sion, Funding acquisition. **Aini Hazwani Shahrir**: Writing - original draft. **Ahmad Nazrul Hakimi Ibrahim**: Formal analysis. **Nor Farah Nadia Ismail**: Formal analysis. **Khairiah Haji Badri**: Writing - review & editing, Supervision.

Declaration of Competing Interest

The authors declare that they have no known competing financial interests or personal relationships that could have appeared to influence the work reported in this paper.

Acknowledgement

The authors would like to express their gratitude to **Universiti Kebangsaan Malaysia** for the financial support for this work (GUP-2018-094).

References

- M. Ameri, S. Nowbakht, M. Molayem, M.H. Mirabimoghaddam, A study on fatigue modeling of hot mix asphalt mixtures based on the viscoelastic continuum damage properties of asphalt binder, *Constr. Build. Mater.* 106 (2016) 243–252, <https://doi.org/10.1016/j.conbuildmat.2015.12.066>.
- G. King, Additives in asphalt, *J. Assoc. Asphalt Paving Technol.* 68 (1999) 32–69.
- T. McNally, in: *Introduction to Polymer modified Bitumen (PMB), Polymer Modified Bitumen*, 2011, pp. 1–21.
- S. Köfteci, P. Ahmedzade, B. Kultayev, Performance evaluation of bitumen modified by various types of waste plastics, *Constr. Build. Mater.* 73 (2014) 592–602, <https://doi.org/10.1016/j.conbuildmat.2014.09.067>.
- M. Liang, X. Xin, W. Fan, H. Sun, Y. Yao, B. Xing, Viscous properties, storage stability and their relationships with microstructure of tire scrap rubber modified asphalt, *Constr. Build. Mater.* 74 (2015) 124–131, <https://doi.org/10.1016/j.conbuildmat.2014.10.015>.
- R. Mistry, T.K. Roy, Effect of using fly ash as alternative filler in hot mix asphalt, *Perspect. Sci.* 8 (2016) 307–309, <https://doi.org/10.1016/j.pisc.2016.04.061>.
- S. Horpibulsuk, M. Hoy, P. Witchayaphong, R. Rachan, A. Arulrajah, Recycled asphalt pavement – fly ash geopolymer as a sustainable stabilized pavement material, *IOP Conf. Ser. Mater. Sci. Eng.* 273 (2017).
- J. Davidovits, Geopolymers – inorganic polymeric new materials, *J. Therm. Anal.* 37 (1991) 1633–1656.
- V.D. Glukhovskiy, Ancient, modern and future concretes, in: P.V. Krivenko (Ed.), *Proc. Fir. Int. Conf. Alka. Cem. Conc.*, 1994, pp. 1–9.
- V.F.F. Barbosa, K.J.D. MacKenzie, Thermal behaviour of inorganic geopolymers and composites derived from sodium polysialate, *Mater. Res. Bull.* 38 (2003) 319–331.
- A. Palomo, F.P. Glasser, Chemically-bonded cementitious material based on metakaolin, *Br. Ceram. Trans. J.* 91 (1992) 107–112.
- H. Xu, J.S.J. Van Deventer, The geopolymerisation of alumino-silicate minerals, *Int. J. Miner. Process.* 59 (2000) 247–266.
- W.M. Kriven, J.L. Bell, M. Gordon, Evaluation of fly ash asphalt, *J. Mater. Civ. Eng.* 227 (2003) 19–25.
- R. Zhao, J.G. Sanjayan, Geopolymer and Portland cement concretes in simulated fire, *Mag. Concr. Res.* 63 (2011) 163–173.
- J.T. Gourley, Geopolymers; opportunities for environmentally friendly construction materials, *Mat. Conf. Ada. Mat. Mod. Soc.*, 2003.
- A.N.H. Ibrahim, N.I. Nur, N. Mohd Akhir, M.N. Borhan, Physical properties and storage stability of geopolymer modified asphalt binder, *J. Teknol.* 78 (2016) 133–138.
- M.Z.N. Khan, F. uddin, A. Shaikh, Y. Hao, H. Hao, Synthesis of high strength ambient cured geopolymer composite by using low calcium fly ash, *Constr. Build. Mater.* 125 (2016) 809–820.
- T. Poltue, A. Suddeepong, S. Horpibulsuk, W. Samingthong, A. Arulrajah, A.S.A. Rashid, Strength development of recycled concrete aggregate stabilized with fly ash-rice husk ash based geopolymer as pavement base material, *Road Mater. Pavement Des.* (2019) 1–12.
- N. Tang, Z. Deng, J.G. Dai, K. Yang, C. Chen, Q. Wang, Geopolymer as an additive of warm mix asphalt: preparation and properties, *J. Clean. Prod.* 192 (2018) 906–915, <https://doi.org/10.1016/j.jclepro.2018.04.276>.
- H. Zain, M.M.A.B. Abdullah, K. Hussin, N. Ariffin, R. Bayuaji, Review on various types of geopolymer materials with the environmental impact assessment, *MATEC Web Conf.* 97 (2017), <https://doi.org/10.1051/mateconf/20179701021>.
- M. Hoy, S. Horpibulsuk, R. Rachan, A. Chinkulkijniwat, A. Arulrajah, Recycled asphalt pavement – fly ash geopolymers as a sustainable pavement base material: strength and toxic leaching investigations, *Sci. Total Environ.* 573 (2016) 19–26.
- M. Hoy, S. Horpibulsuk, A. Arulrajah, Strength development of recycled asphalt pavement – fly ash geopolymer as a road construction material, *Constr. Build. Mater.* 117 (2016) 209–219.
- A.N.H. Ibrahim, F.H. Khairuddin, N.I. Md Yusoff, M.N. Borhan, N. Mohd Akhir, Sifat mekanik dan tingkah laku resapan air bitumen terubahsuai geopolimer, *J. Teknol.* 79 (2017) 107–111.
- N. Ali, J.S. Chan, S. Simms, R. Bushman, A.T. Bergan, Mechanistic evaluation of fly ash asphalt, *J. Mater. Civ. Eng.* 8 (1996) 19–25.
- N.B. Singh, Fly ash-based geopolymer binder: a future construction material, *Minerals* 8 (2018), <https://doi.org/10.3390/min8070299>.
- A.N.H. Ibrahim, N.I.M. Yusoff, N.M. Akhir, M.N. Borhan, Physical properties and storage, stability of geopolymer modified asphalt binder, *J. Teknol. (Sci. Eng.)* 78 (2016) 133–138.
- A. Kusiantoro, M.S. Ibrahim, K. Muthusamy, A. Alias, Development of sucrose and citric acid as the natural based admixture for fly ash based geopolymer, *Proc. Environ. Sci.* 17 (2013) 596–602, <https://doi.org/10.1016/j.proenv.2013.02.075>.
- G. Reena, K. Verinder, Characterization of bitumen and modified bitumen (e-mpb) using FT-IR, thermal and SEM techniques, *Res. J. Chem. Sci.* 2 (2012) 2231–2606.
- A.W. Hefner, D.N. Little, R.L. Lytton, I.L. Al-Qadi, M. Taylor, G. King, D. Anderson, A synthesis of theories and mechanisms of bitumen-aggregate adhesion including recent advances in quantifying the effects of water, *Asphalt Paving Technol. Assoc. Asphalt Paving Technol. Tech. Sess.* 74 (2005) 139–195.
- S. Hj, M.A. Tarawneh, S.Y. Yahya, R. Rasi, Reinforced thermoplastic natural rubber (TPNR) composites with different types of carbon nanotubes (MWNTS), *Carbon Nanotube Synth. Charact. Appl.* (2011).
- K.A. Mat Amin, K. Haji Badri, Palm-based bio-composites hybridized with kaolinite, *J. Appl. Polym. Sci.* 105 (5) (2007) 2658–2667.
- T.W. Cheng, J.P. Chiu, Fire-resistant geopolymer produce by granulated blast furnace slag, *Miner. Eng.* 16 (2003) 205–210.
- J.R.A. Grenfell, N. Ahmad, Y. Liu, A.K. Apeagyei, G.D. Airey, D. Large, Application of surface free energy techniques to evaluate bitumen-aggregate bonding strength and bituminous mixture moisture sensitivity, *Proc. Inst. Civ. Eng. Constr. Mater* 167 (2014) 214–226.
- E. Sina, E. Cyrus, in: *Surface Treatment of Materials for Adhesive Bonding*, 2006, pp. 95–154.
- R.C. Kwok, D. Vogel, Assessment Challenges and Solutions, 1999.
- M.A. Hubbe, D.J. Gardner, W. Shen, Contact angles and wettability of cellulosic surfaces: a review of proposed mechanisms and test strategies, *BioResources*. 10 (2015) 8657–8749.
- F.M. Fowkes, Contact angle, wettability, and adhesion, copyright, *Adv. Chem. Ser.* (1964) i–iii.
- S. Liu, X. Yu, F. Dong, Evaluation of moisture susceptibility of foamed warm asphalt produced by water injection using surface free energy method, *Constr. Build. Mater.* 131 (2017) 138–145, <https://doi.org/10.1016/j.conbuildmat.2016.11.072>.
- A. Habal, D. Singh, Moisture damage resistance of GTR-modified asphalt binders containing WMA additives using the surface free energy approach, *J. Perform. Constr. Facil.* 31 (2017) 04017006, [https://doi.org/10.1061/\(ASCE\)CF.1943-5509.0000995](https://doi.org/10.1061/(ASCE)CF.1943-5509.0000995).
- A.T. Pauli, J.F. Branthaver, R.E. Robertson, W. Grimes, C.M. Eggleston, Atomic force microscopy investigation of SHRP asphalt: heavy oil and resid compatibility and stability, *Pre. Am. Chem. Soc. Div. Pet. Chem.* 46 (2) (2001) 104–110.
- L. Loeber, O. Sutton, J. Morel, J.M. Valleton, G. Muller, New direct observations of asphalt and asphalt binders by scanning electron microscopy and atomic force microscopy, *J. Microsc.* 182 (1996) 32–39.
- L. Loeber, G. Muller, J. Morel, O. Sutton, Bitumen in colloid science: a chemical, structural and rheological approach, *Fuel* 77 (1998) 1443–1450.
- B. Li, J. Liu, F. Han, X. Li, L. Li, Y. Li, X. Duan, Preparation of flame retardant modified with titanate for asphalt binder, *Adv. Mater. Sci. Eng.* 2014 (2014) 8. ID 510958.
- X. Yu, N.A. Burnham, R.B. Mallick, M. Tao, A systematic AFM-based method to measure adhesion differences between micron-sized domains in asphalt binders, *Fuel* 113 (2013) 443–447.
- J.F. Masson, V. Leblond, J. Margeson, Bitumen morphologies by phase-detection atomic force microscopy, *J. Microsc.* 221 (2006) 17–29, <https://doi.org/10.1111/j.1365-2818.2006.01540.x>.
- B. Mccarron, X. Yu, M. Tao, N. Burnham, The Investigation of ‘Bee-Structures’ in Asphalt Binders, 2012.

Investigation of the chemical, strength, adhesion

ORIGINALITY REPORT

16%

SIMILARITY INDEX

%

INTERNET SOURCES

16%

PUBLICATIONS

%

STUDENT PAPERS

MATCH ALL SOURCES (ONLY SELECTED SOURCE PRINTED)

2%

★ Hend Ali Omar, Nur Izzi Md. Yusoff, Halil Ceylan, Irman Abdul Rahman, Zainuddin Sajuri, Fauzan Mohd Jakarni, Amiruddin Ismail. "Determining the water damage resistance of nano-clay modified bitumens using the indirect tensile strength and surface free energy methods", Construction and Building Materials, 2018

Publication

Exclude quotes On

Exclude matches Off

Exclude bibliography On